

Scanning probe microscopy techniques for mechanical characterization at nanoscale

D. PASSERI⁽¹⁾(*), P. ANASTASIADIS⁽²⁾(³), E. TAMBURRI⁽⁴⁾, V. GUGLIELMOTTI⁽⁴⁾
and M. ROSSI⁽¹⁾(⁵)

⁽¹⁾ *Department of Basic and Applied Sciences for Engineering, University of Rome Sapienza, and Electron Microscopies and Nanoscopies Laboratory (EMINA lab) - Via A. Scarpa 16, 00161 Rome, Italy*

⁽²⁾ *Department of Molecular Biosciences and Bioengineering, University of Hawaii - Honolulu, HI 96822, USA*

⁽³⁾ *Department of Mechanical Engineering, University of Hawaii - Honolulu, HI 96822, USA*

⁽⁴⁾ *Department of Chemical Sciences and Technologies, University of Rome Tor Vergata, and Micro and Nano-structured Systems Laboratory (MINAS lab) - Via della Ricerca Scientifica, 00133 Rome, Italy*

⁽⁵⁾ *Centro di Ricerca per le Nanotecnologie Applicate all'Ingegneria della Sapienza (CNIS), University of Rome Sapienza - Piazzale A. Moro 5, 00185 Rome, Italy*

ricevuto il 19 Febbraio 2013

Summary. — Three atomic force microscopy (AFM)-based techniques are reviewed that allow one to conduct accurate measurements of mechanical properties of either stiff or compliant materials at a nanometer scale. Atomic force acoustic microscopy, AFM-based depth sensing indentation, and torsional harmonic AFM are briefly described. Examples and results of quantitative characterization of stiff (an ultrathin SeSn film), soft polymeric (polyaniline fibers doped with detonation nanodiamond) and biological (collagen fibers) materials are reported.

PACS 68.37.Ps – Atomic force microscopy (AFM).

PACS 62.20.de – Elastic moduli.

PACS 68.60.Bs – Mechanical and acoustical properties.

PACS 82.35.Lr – Physical properties of polymers.

1. – Introduction

The progress in nanoscience and nanotechnology is accompanied by a need for accurate techniques facilitating the investigation of physical and chemical properties of

(*) E-mail: daniele.passeri@uniroma1.it

materials at the nanoscale [1]. In particular, methodologies for a mechanical characterization of materials in a wide range of Young's moduli are required, from stiff coatings to compliant polymers and biological specimens. These techniques should ideally allow for the accurate determination of mechanical properties at regions of interest at a lateral resolution in the nanoscale, as well as the simultaneous morphological and mechanical imaging of the surface. To this aim, atomic force microscopy (AFM) represents a powerful technique for the development of mechanical single-point measurements and imaging techniques. This is largely due to its unique capabilities of scanning the surface at a nanometer resolution in combination with the possibility of exerting ultra-low loads on the sample surface. In this study, we briefly review the AFM-based techniques for the mechanical characterization of surfaces that have been developed and are available at EMINA [2] and CNIS [3] laboratories. Despite the fact that numerous other AFM methodologies have been described extensively in the literature [4,5], the techniques described in this review enable the study of stiff and compliant materials, *i.e.*, where the Young's modulus ranges from a few hundreds of gigapascals to a few tens of megapascals. In particular, soft samples can be probed down to different penetration depths, which permits the investigation of both bulk and near surface mechanical properties.

2. – Characterization of stiff materials

2.1. Atomic force acoustic microscopy. – In atomic force acoustic microscopy (AFAM) the tip remains in contact with the surface of the sample, whose back side is coupled to an out-of-plane oscillating ultrasonic transducer. Ultrasonic waves induce vibrations in the entire system composed by the cantilever, the tip, and the material in a small volume positioned under the tip. As a result, a high-frequency oscillating component is present in the cantilever deflection signal. The resonances of the system can be detected by sweeping the excitation frequency of the transducer. Such resonances are generally referred to as the contact resonance frequencies (CRFs) of the cantilever and are related to the mechanical properties of the sample: the stiffer the sample, the higher the CRFs. CRFs can be acquired simultaneously with the standard morphological reconstruction. Thus the obtained images reflect the local elastic properties of the sample. CRFs can be eventually analyzed to deduce the sample indentation modulus M through the following procedure: i) a suitable model for the system has to be assumed, *e.g.*, describing the cantilever as a uniform beam and the tip-sample contact as a spring with constant k^* (namely, the tip-sample contact stiffness), and then ii) the unknown geometrical properties of the tip have to be calibrated on a reference sample. AFAM has been demonstrated to enable accurate single-point measurements on several stiff materials, both bulk and thin films [6,7], as well as quantitative indentation modulus mapping [8-10]. As an example, fig. 1 shows the AFAM characterization of a 22 nm thick SeSn ultrathin film thermally deposited on quartz substrates using our AFM apparatus (Solver, NT-MDT, Russia) equipped with a standard Si cantilever (NSC16, Mikromasch, Estonia) [11]. In the topographical image (fig. 1a) grains are visible that appear darker (*i.e.*, softer) compared to the surrounding material in the first and second CRF images (fig. 1b and c, respectively). After calibration using the quartz substrate as the reference, fig. 1b and c can be used to retrieve the quantitative map of the indentation modulus of the film-substrate system (fig. 1d). Indeed, due to the low thickness of the film, the measured value of M is the composition of the moduli of the film and the substrate [11]. The obtained values for M (fig. 1d) reveal that the stiffer region exhibits modulus values in the range of 60–70 GPa and stands therefore in good agreement with previously reported results [11]. Conversely, the softer

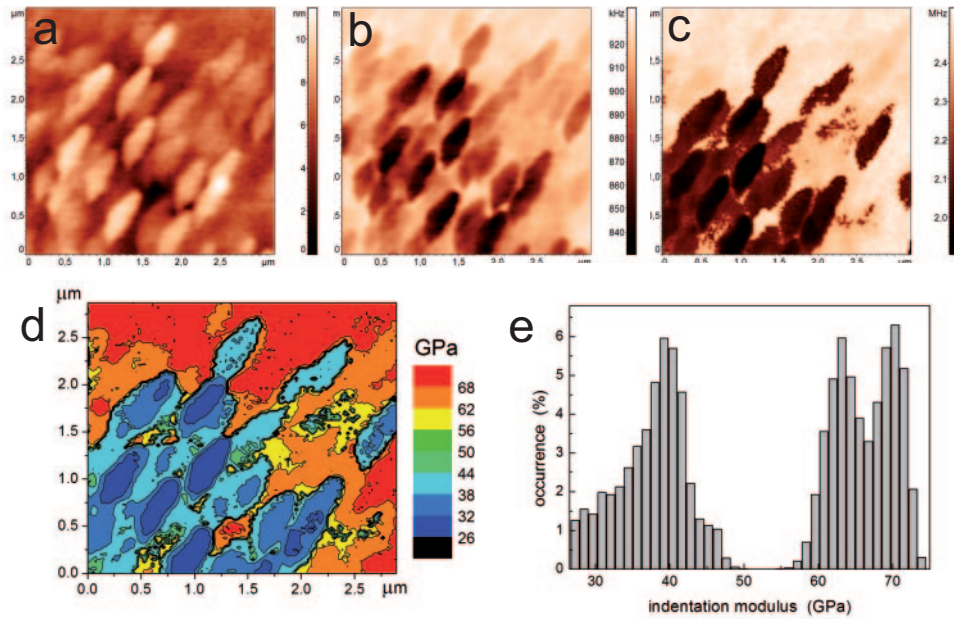


Fig. 1. – AFAM characterization of SeSn ultrathin film: (a) topography; (b) first and (c) second contact resonance frequency images; (d) map of the indentation modulus; (e) statistics of the indentation modulus values from (d).

region has indentation modulus values around 40 GPa, which the higher thickness of the film does not completely account for, and that could indicate the presence of amorphous material. Moreover, the possibility of poor adhesion and/or presence of voids between such material and the underlying film should be accounted for as it may further reduce the apparent indentation modulus [12, 13].

3. – Characterization of compliant materials

3.1. AFM quasi-static indentation. – The AFM cantilever can be used as an indenter to record force *versus* indentation curves on compliant samples [14]. By varying the maximum applied load and depending on the elastic modulus of the probed sample, different penetration depths can be achieved from few to several tens or even a few hundreds of nanometers. Since lack of knowledge about the exact geometry of the tip is the main limiting factor, we developed an approach that uses a set of reference samples to compensate for accuracy. The indentation moduli of the reference materials set the calibration range for this technique [15, 16]. Our approach has been used to characterize different polymeric thin films deposited on stiff substrates, such as poly(3,4-ethylenedioxythiophene) (PEDOT) doped with poly(4-styrenesulfonate) (PSS) with thickness of 300 nm and polyaniline (PANI) with thickness from 150 nm to 280 nm [16, 17]. In order to illustrate our technique, we report the characterization of the radial indentation modulus of collagen fibers in human breast cancer cells. Cells from the MCF-7 breast cancer cell line were cultured in Eagle's Minimum Essential Medium supplemented by 10% fetal bovine serum (ATCC, Manassas, VA, USA) and 0.01 mg/mL bovine insulin (Invitrogen, Grand Island,

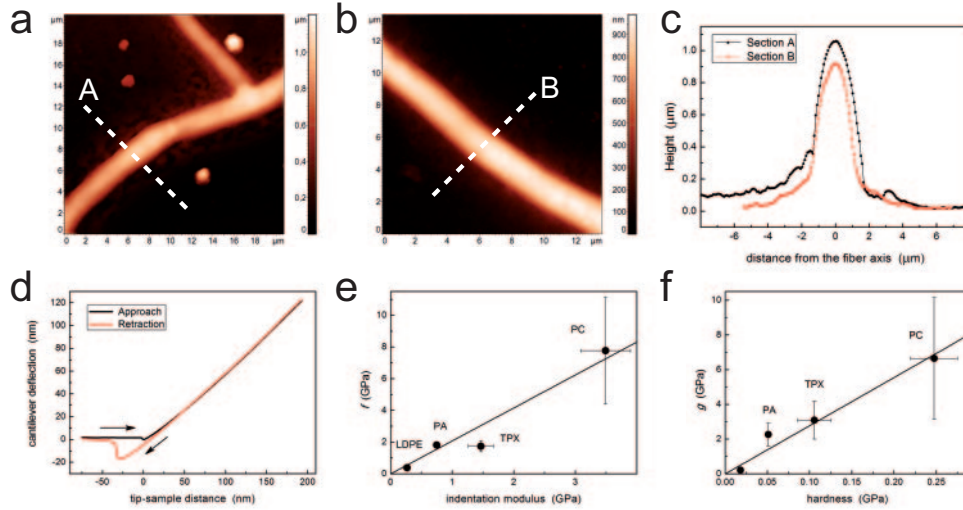


Fig. 2. – Characterization of collagen fibers using AFM quasi-static indentation: (a) and (b) topographical images of two investigated fibers, the one in (b) being measured 5 months later than that in (a); (c) profiles of the two investigated fibers; (d) typical cantilever deflection versus tip-sample distance curve acquired on the axis of the fiber in (b); calibration curves for the determination of the indentation modulus (e) and hardness (f).

NY, USA). The cells were kept in standard 75 cm² cell culture flasks and incubated at 37 °C in a humidified atmosphere with 5% CO₂ and 95% relative humidity. Prior to the experimental assays the cells were detached from the culture flasks by enzymatic reaction using 0.25% (w/v) Trypsin - 0.53 mM EDTA in Hank's balanced salt solution without Ca⁺⁺ and Mg⁺⁺ (ATCC, Manassas, VA, USA). The reaction was neutralized by addition of complete cell growth culture medium. Subsequently, the cells were transferred to a LabTek™ II chambered coverglass and placed back to the CO₂ cell incubator (Nunc, Rochester, NY, USA). After 24 hours the MCF-7 cells were dried under a mild nitrogen air stream in preparation for the AFM characterizations. AFM experiments were performed using our AFM apparatus (Solver, NT-MDT, Russia) equipped with standard Si cantilevers (NSG10 and NSG01, NT-MDT, Russia). In fig. 2a the probed collagen fiber can be seen. After keeping the sample under room conditions for five months, measurements were repeated on the fiber shown in fig. 2b. The two fibers exhibit similar characteristics, with diameters of 1 and 0.9 μm, respectively (see their profile sections reported in fig. 2c). In each measurement session, several cantilever deflection *versus* tip-sample distance curves were collected at different locations on the collagen fiber axis, like the one shown in fig. 2d. From each curve, two parameters are evaluated, namely, f and g , which are proportional to M and to the indentation hardness H , respectively [15, 16]. For calibration purposes, in the same measurement session f and g have been evaluated for a set of four polymeric samples used as references, *i.e.*, low-density polyethylene (LDPE), polyamide (PA), polymethylpentene (TPX), and polycarbonate (PC), whose M and H were previously determined by standard indentation [16]. As an example, the $f(M)$ and $g(H)$ calibration curves relative to the characterization of the collagen fiber in fig. 2b are reported in fig. 2e and 2f, respectively. M and H of the collagen fiber were measured as high as $M = 2.1 \pm 0.9$ GPa and $H = 160 \pm 60$ MPa in the

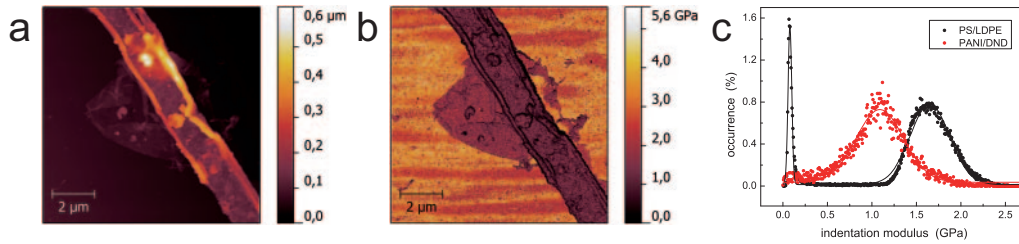


Fig. 3. – TH-AFM characterization of a PANI/DND fiber: topographical image (a) and corresponding indentation modulus map (b); (c) indentation modulus values measured on the fiber compared to those measured on the PS/LDPE reference sample (symbols) together with the corresponding Gaussian fit (solid lines).

first measurement session, in agreement with data reported in literature [18, 19]. After 5 months, $M = 0.40 \pm 0.15$ GPa and $H = 40 \pm 20$ MPa were found. The decreased values are explained due to dehydration and ageing [20].

3'2. Torsional harmonic AFM. – In torsional harmonic AFM (TH-AFM), the surface of a sample is imaged in tapping mode using a T-shaped cantilever with out-of-axis tip at its first flexural resonance f_0 [21]. When a compliant material is imaged, the tip periodically indents the surface. Due to the displacement of the tip from the axis, during the tip-sample contact a torque is exerted on the cantilever resulting in the periodical variation of the cantilever torsion signal [21]. The latter can be reconstructed via inverse Fourier transform having acquired its harmonic components at frequencies $N \times f_0$ (N from 1 to about 20). The cantilever torsion signal can be then filtered to extract the cantilever deflection *versus* tip-sample distance curve [21]. Quantitative force *versus* distance curves can be obtained after force calibration using a stiff sample. Such curves can be used to quantify the sample indentation modulus after calibration of the tip radius using a reference sample. Thus, simultaneously to standard topography and phase images, maps can be collected of sample indentation modulus, maximum applied load, tip-sample adhesion, and dissipation during an indentation cycle. The accuracy of TH-AFM has been demonstrated for materials with elastic modulus ranging from a few tens of megapascals to a few gigapascals [22]. As an example, we report the characterization of nanostructured polymeric fibers, obtained by chemical polymerization of polyaniline (PANI) in presence of detonation nanodiamond (DND) nanoparticles and collected on monocrystalline Si substrates. Measurements were performed using our AFM apparatus (Dimension Icon, Bruker Inc.) equipped with a T-shaped cantilever (HMX10, Bruker Inc.). Figure 3a shows the morphological reconstruction of a typical PANI/DND fiber. Figure 3b shows the corresponding quantitative map of indentation modulus after calibration using a blend of LDPE (M about 100 MPa) and polystyrene (PS, $M = 1.6$ GPa) as the reference sample (PS/LDPE calibration sample by Bruker Inc.). The indentation modulus of the bright area (corresponding to the stiff Si substrate) is not significant, being out of the calibration range. Conversely, the indentation modulus map can be considered accurate in correspondence of the PANI/DND fiber, since the measured values are in the calibration range. Figure 3c shows the statistics of the indentation modulus values measured on the PANI/DND fiber and on the PS/LDPE reference sample, from which the indentation modulus of the PANI/DND fiber can be evaluated as high as 1.1 ± 0.5 GPa.

4. – Conclusion

Three AFM-based techniques for the mechanical characterization of material at the micro and nanometer scale have been illustrated, which are currently available at EMINA/CNIS laboratories, *i.e.*, atomic force acoustic microscopy, AFM-based quasi-static indentation and torsional harmonic AFM. Altogether, such techniques allow us to accurately investigate materials in a wide range of indentation modulus values, from stiff samples with modulus as high as a few hundreds of gigapascals to polymeric and biological materials with modulus as low as few tens of megapascals.

REFERENCES

- [1] LEACH R. K., BOYD R., BURKE T., DANZEBRINK H. U., DIRSCHERL K., DZIOMBA T., GEE M., KOENDERS L., MORAZZANI V., PIDDUCK A., ROY D., UNGER W. E. S. and TACOOT A., *Nanotechnology*, **22** (2011) 062001.
- [2] <http://w3.uniroma1.it/emina/>.
- [3] <http://w3.uniroma1.it/sapienzanano/>.
- [4] MARINELLO F., PASSERI D. and SAVIO E. (Editors), *Acoustic scanning probe microscopy* (Springer, Berlin, Heidelberg) 2012.
- [5] PASSERI D., ROSSI M., TAMBURRI E. and TERRANOVA M. L., *Anal. Bioanal. Chem.*, **405** (2013) 1463.
- [6] HURLEY D. C., KOPYCINSKA-MÜLLER M. and KOS A. B., *JOM*, **59** (2007) 23.
- [7] PASSERI D., BETTUCCI A., GERMANO M., ROSSI M., ALIPPI A., ORLANDUCCI S., TERRANOVA M. L. and CIAVARELLA M., *Rev. Sci. Instrum.*, **76** (2005) 093904.
- [8] HURLEY D. C., KOPYCINSKA-MÜLLER M., KOS A. B. and GEISS R. H., *Adv. Eng. Mater.*, **7** (2005) 713.
- [9] PASSERI D., BETTUCCI A., GERMANO M., ROSSI M., ALIPPI A., SESSA V., FIORI A., TAMBURRI E. and TERRANOVA M. L., *Appl. Phys. Lett.*, **88** (2006) 121910.
- [10] KUMAR A., RABE U. and ARNOLD W., *Jpn. J. Appl. Phys.*, **47** (2008) 6077.
- [11] PASSERI D., ROSSI M., ALIPPI A., BETTUCCI A., MANNO D., SERRA A., FILIPPO E., LUCCI M. and DAVOLI I., *Superlattices Microstruct.*, **44** (2008) 641.
- [12] HURLEY D. C., KOPYCINSKA-MÜLLER M., LANGLOIS E. D. and BARBOSA III N., *Appl. Phys. Lett.*, **89** (2006) 021911.
- [13] PARLAK Z. and DEGERTEKIN F. L., *J. Appl. Phys.*, **103** (2008) 114910.
- [14] BUTT H. J., CAPPELLA B. and KAPPL M., *Surf. Sci. Rep.*, **59** (2005) 1.
- [15] PASSERI D., BETTUCCI A., BIAGIONI A., ROSSI M., ALIPPI A., LUCCI M., DAVOLI I. and BEREZINA S., *Rev. Sci. Instrum.*, **79** (2008) 066105.
- [16] PASSERI D., BETTUCCI A., BIAGIONI A., ROSSI M., ALIPPI A., TAMBURRI E., LUCCI M., DAVOLI I. and BEREZINA S., *Ultramicroscopy*, **109** (2009) 1417.
- [17] PASSERI D., ALIPPI A., BETTUCCI A., ROSSI M., ALIPPI A., TAMBURRI E. and TERRANOVA M. L., *Synth. Met.*, **161** (2011) 7.
- [18] YANG L., VAN DER WERF K. O., FITIÉ C. F. C., BENNINK M. L., DIJKSTRA P. J. and FEIJEN J., *Biophys. J.*, **94** (2008) 2204.
- [19] HEIM A. J., MATTHEWS W. G. and KOOB T. J., *Appl. Phys. Lett.*, **89** (2006) 181902.
- [20] BAILEY A. J., *Mech. Ageing Dev.*, **122** (2001) 735.
- [21] SAHIN O., MAGONOV S., SU C., QUATE C. F. and SOLGAARD O., *Nat. Nanotechnol.*, **2** (2007) 507.
- [22] SAHIN O. and ERINA N., *Nanotechnology*, **19** (2008) 445717.